2014 SCEC Report

Laboratory Experiments on Fault Shear Resistance Relevant to Coseismic Earthquake Slip

PI:

Terry E. Tullis, Brown University

SUMMARY

After focusing our attention for several years on silica-gel weakening [*Di Toro et al.*, 2004; *Goldsby and Tullis*, 2002] and flash weakening [*Beeler et al.*, 2008; *Goldsby and Tullis*, 2011; *Kohli et al.*, 2011; *Rice*, 2006] we have turned our attention to the widely discussed dynamic weakening mechanism termed *thermal pore-fluid pressurization,* hereafter abbreviated as TP. There are many theoretical and numerical studies of TP [*Andrews*, 2002; *Lachenbruch*, 1980; *Lee and Delaney*, 1987; *Mase and Smith*, 1985; 1987; *Noda*, 2008; *Noda and Shimamoto*, 2005; *Rempel and Rice*, 2006; *Rice*, 2006; *Rice and Cocco*, 2007; *Sibson*, 1973] and it is increasingly used in dynamic rupture and earthquake nucleation models [*Bizzarri and Cocco*, 2006a; b; *Lapusta and Rice*, 2004a; b; *Noda et al.*, 2009; *Noda and Lapusta*, 2010; *Rice et al.*, 2010; *Schmitt and Segall*, 2009; *Segall and Rice*, 2006]. However, experimental data suggesting the operation of this mechanism is limited, a shortcoming we are working to resolve via this and related research.

From 2003 to 2013 this laboratory friction work was funded by SCEC via a grant to Brown in which Terry Tullis and David Goldsby were the PIs. After the July 2014 departure of David Goldsby to the University of Pennsylvania, Terry Tullis and an outstanding postdoc, Keishi Okazaki, are continuing this work at Brown. The only machine in existence capable of doing the required experiments is our unique high-pressure rotary shear friction machine that combines arbitrarily large slip displacement with independent control of both confining pressure and flow-through pore pressure capability. Ours is the first study in which the thermal pressurization mechanism has been isolated and is beginning to be characterized under controlled conditions on confined samples (e.g., with fully saturated rocks of controlled fluid pressure and proscribed permeabilities of the rock samples). Note that this work has been partly funded by the USGS NEHRP external program, so it is the combination of the USGS and SCEC support that allows this work to be done.

We have developed a successful protocol for thermally cracking our initially low permeability Frederick diabase samples ($<10^{-23}$ m^2) and measuring the resulting permeabilities in the 10^{-23} m^2 to 10^{-18} m^2 range. This is a rock that does not undergo weakening due to silicate gel formation or other dynamic weakening mechanisms at the relatively high slip rates and meters of slip of our experiments. We have conducted finite element model (FEM) calculations of the temperatures achieved in our experiments. To verify the FEM calculations and calibrate the values of thermal conductivities used, we have made direct measurements of temperature by placing a thermocouple in a hole drilled to within a fraction of a mm of the sliding surface. These measurements entail a tedious procedure of running tiny thermocouple wires through our capillary pore pressure tubing and out through a pressure seal in the pore pressure system. We have been successful in activating thermal pressurization in our experiments as comparison of our mechanical and thermal results with theoretical predictions make clear.

TECHNICAL REPORT

In last year's report we presented some results of our FEM measurements and a comparison of the mechanical weakening with theoretical predictions for thermal pressurization by [*Rice*, 2006]. In this report we focus on experimental data collected during the past year in which we have verified our FEM modeling with direct temperature measurements.

Experiments were conducted on samples fully saturated before frictional sliding. Because of the low permeability of the diabase rings, a relatively high pore pressure must be applied to the samples to saturate them in a practical amount of time. Saturation thus had to be accomplished with the samples subjected to relatively large pore pressures while confined in the high-pressure apparatus. The following procedure was therefore developed: 1) samples were pressurized in the gas apparatus, 2) a constant pore pressure was applied to the lower sample grip, 3) pore pressure was held constant until water could be seen exiting the sample assembly from the pore-pressure tubing connected to the upper sample ring, 4) the sample was depressurized and the pore-pressure port on the bottom sample grip was plugged (the flow-through tubing used during saturation is incompatible with the large sliding displacements, meters of slip, of our thermal pressurization tests), 5) the sample was repressurized to the testing confining pressure and the desired pore pressure of the run conditions was applied, and 6) sliding was commenced after the externally applied pore pressure was equilibrated throughout the sample (i.e., after no movement of the pore pressure piston into the pore pressure cylinder was observed). In the experiment described below we used a confining pressure of 45 MPa, an applied normal stress of 50 MPa, and a fluid pressure of 25 MPa, yielding an effective normal stress of 25 MPa. (Due to the low permeability of the sample, fluid pressure within the fault zone may deviate significantly from the applied value when fluid pressure changes rapidly on the fault). For this experiment the permeability was unfortunately somewhat higher than the one described in last year's report and therefore little weakening due to thermal pressurization occurred.

The experiment shown in Figure 1 experienced 4 periods of successively higher sliding velocities, preceded and separated by sliding at 1 micron/s. As shown in the blue curve, these increased velocities were 0.6, 1.2, 2.4 and 4.8 mm/s. The green curve shows the motion of the two fault surfaces normal to one another, with convergence being positive. The periodic oscillations of the green curve have a period of one revolution of the sample and correspond to 155 mm of slip. They presumably occur because the two surfaces are not perfectly normal to the axis of rotation, in spite of great care to try to make them so. Greater convergence should correspond to angular positions where the tilt of the rotating surface matches that of the stationary surface so they are more parallel, and greater divergence when the surfaces are tilted in opposite directions creating a less uniform distribution of normal stress around the circumference. Note that the apparent period on the time abscissa decreases by a factor of 2 as the speed successively doubles. Note also the increases in temperature each time the velocity goes from 1 μm/s to the higher speeds and the decay when the velocity returns to 1 μm/s. As expected, successively higher speeds produce successively higher temperatures and the average of the measured values match the FEM calculated values. The periodic oscillations of the measured temperature with the period of revolution of the sample are notable and the temperature highs presumably correspond to times of highest normal stress at the thermocouple location. With the exception of the first cycle at 0.6 mm/s, the peaks of the temperature are in phase with the peaks in the convergence of the surfaces. Presumably there would be a phase shift from this for a thermocouple located at some other position around the circumference. The thermocouple is embedded in the stationary upper sample and the in-phase behavior between convergence and temperature suggests that the thermocouple happens to be located at nearly the location around the circumference on the upper grip where the sample projects the least from the grip so that it feels less normal stress when the surfaces are not parallel – if it were located on the

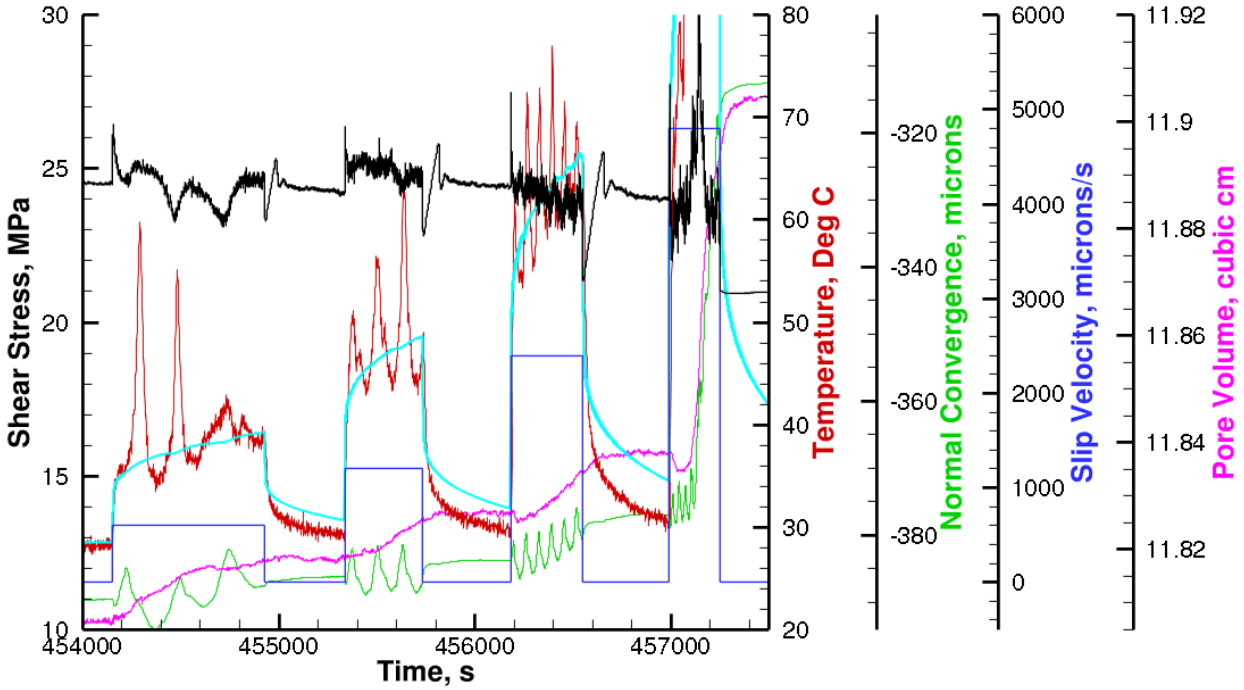

Figure 1. Overall view of the high velocity portion of experiment on diabase with a permeability of ~2×10^{-18} m^2, and a thermocouple embedded just below the sliding surface. A number of interrelated variables are plotted. The colors of the titles on the axes correspond to the color of the line being plotted. Temperatures measured are in red and calculated via FEM are in cyan – note their good agreement for each velocity step. See text for discussion of the several interesting features that can be seen.

part that projected the most it would feel more normal stress when the surfaces were separated and the temperature peaks would be in-phase with the convergence lows.

In addition to the obvious correlations just pointed out, there are other notable ones. Not shown on this plot due to the large number of other variables we wanted to show, the confining pressure increases during the periods of rapid sliding and hence greater shear heating and decreases when the velocity is low and cooling can occur. Although we servo to keep the confining pressure constant, this is only done by adding gas to compensate for continual slow leaks and so increases in gas confining pressure due to thermal expansion are not compensated for by any removal of gas. A more subtle behavior, but particularly significant from the perspective of thermal pressurization, is that of the pore volume shown in the magenta curve. This is a measure of how much volume of pore fluid is added to or subtracted from the pore pressure tubing to maintain a constant pore pressure on the outer surfaces of the low permeability rock. Due to the low permeability of the sample and the fact that we measure the pore pressure in high-pressure tubing external to the pressure vessel, we do not have a direct measure of the pore pressure in the sample. However, during the rapid slip, the pore volume initially decreases, meaning that elevated pore pressure is building up in the sample and the permeability is high enough that some of that increase is being felt by the external pore-pressure transducer. Since we are servoing to keep the external pore pressure constant, the pore pressure intensifier withdraws. This is most visible immediately following the start of the 2.4 and 4.8 mm/s velocity steps (see also Figure 2). Note, however, that except for this initial response to an increase in pore pressure along the fault surface, the pore volume primarily increases during the periods of increasing velocity. This is

unexpected and the only explanation we have for it at present is cracking in the sample causing dilatancy. Although there is some correlation with the normal convergence, the correlation is only strong at 2.4 mm/s and there is no correlation with the periodic oscillations of convergence.

Two notable aspects of this data set have not been addressed in the above discussion. One is that at 4.8 mm/s after 2 or 3 revolutions (300 to 500 mm of slip) the sample appears to have degraded, possibly undergoing some substantial fracturing. The shear stress increased much more than during the lower speed steps and especially the normal convergence and the pore volume channels underwent unprecedented upward excursions. At about the time this was all happening the thermocouple suddenly stopped sending a signal, presumably because the surface had worn down to the level of the thermocouple junction, or a fracture in the rock separated the wires. At this point the experiment was over, although the data to that point are excellent.

The second notable aspect of the data set is that there is very little decrease in the shear strength associated with the increases in slip velocity and increase in temperature. This is in clear contrast to the substantial weakening shown in the experiment described in last year's report. The obvious reason for this is that the permeability in this sample is higher than in that experiment by nearly an order of magnitude. So although the temperature rose sufficiently to cause the pore fluid to expand, as the above discussion makes clear, the hydraulic diffusivity was sufficiently high that very little increase in pore pressure was apparently allowed to build up. As shown in Figure 2, a blow-up and somewhat rescaled version of the 2.4 mm/s portion of Figure 1, there is an increase in the shear stress when going from 0.001 mm/s to 2.4 mm, which might be a standard rate and state friction direct effect. This is followed by a decay back to about the level of shear stress that existed while sliding at 0.001 mm/s. However, this cannot be a typical rate and state friction evolution-effect decay because it takes place over a period of ~12 seconds which corresponds to ~30 mm of slip, a distance very much longer than the few-micron Dc for rate and state friction, and is presumably due to thermal pressurization.

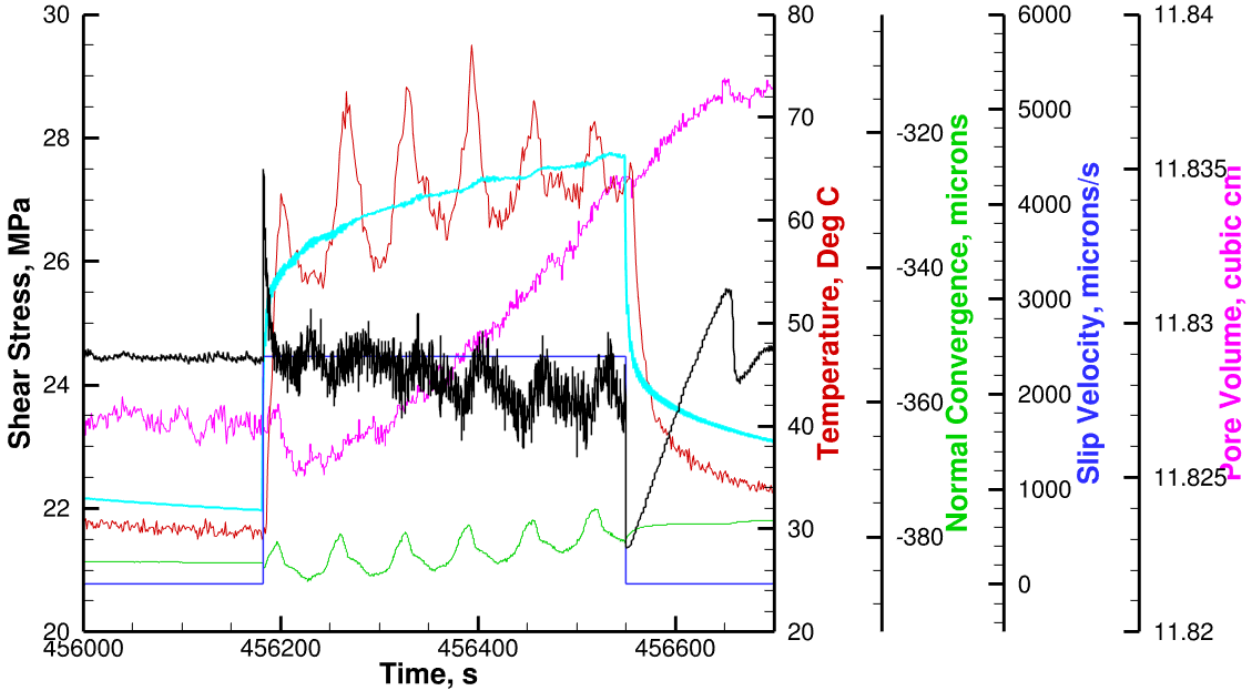

Figure 2. Detail of the behavior of the experiment shown in Figure 1 for the segment during which the slip velocity was raised to 2.4 mm/s. See text for discussion.

Intellectual Merit

The research contributes to our understanding of the earthquake energy budget, strong ground motions, and accelerations associated with earthquake faulting, by providing fundamental knowledge of the coseismic shear resistance of faults.

Broader Impacts

Results of our experiments are incorporated in coursework at Brown. The experiments have provided new sample fixtures and other enhancements to existing equipment that enhance the infrastructure for research and education. Society benefits from an acquisition of scientific knowledge and in improved understanding of earthquakes and how to mitigate their damage.

REFERENCES CITED

Andrews, D. J. (2002), A fault constitutive relation accounting for thermal pressurization of pore fluid, *J. Geophys. Res.*, *107*, 12.

Beeler, N. M., T. E. Tullis, and D. L. Goldsby (2008), Constitutive relationships and physical basis of fault strength due to flash-heating, *J. Geophys. Res.*, *113*, B01401, doi:01410.01029/02007JB004988.

Bizzarri, A., and M. Cocco (2006a), A thermal pressurization model for the spontaneous dynamic rupture propagation on a three-dimensional fault: 1. Methodological approach, *J. Geophys. Res.*, *111*, B05303, doi:05310.01029/02005JB003862.

Bizzarri, A., and M. Cocco (2006b), A thermal pressurization model for the spontaneous dynamic rupture propagation on a three-dimensional fault: 2. Traction evolution and dynamic parameters, *J. Geophys. Res.*, *111*, B05304, doi:05310.01029/02005JB003864.

Di Toro, G., D. L. Goldsby, and T. E. Tullis (2004), Friction falls toward zero in quartz rock as slip velocity approaches seismic rates, *Nature*, *427*, 436-439.

Goldsby, D. L., and T. E. Tullis (2002), Low frictional strength of quartz rocks at subseismic slip rates, *Geophys. Res. Lett.*, *29*(17), 1844, doi:1810.1029/2002GL015240.

Goldsby, D. L., and T. E. Tullis (2011), Flash heating leads to low strength of crustal rocks at earthquake slip rates, *Science*, *334*, 216-218, DOI: 210.1126/science.1207902.

Kohli, A. H., D. L. Goldsby, G. Hirth, and T. E. Tullis (2011), Flash weakening of serpentinite at near-seismic slip rates, *J. Geophys. Res.*, *116, B03202*, doi:10.1029/2010JB007833.

Lachenbruch, A. H. (1980), Frictional heating, fluid pressure, and the resistance to fault motion, *J. Geophys. Res.*, *85*, 6249-6272.

Lapusta, N., and J. R. Rice (2004a), Earthquake sequences on rate and state faults with strong dynamic weakening, *Eos. Trans. Am. Geophys. Union, Fall Meeting Suppl.*, *85*(47), T22A-05.

Lapusta, N., and J. R. Rice (2004b), Earthquake sequences on rate and state faults with strong dynamic weakening, paper presented at 2004 SCEC Annual Meeting Proceedings and Abstracts, Southern California Earthquake Center, PalmSprings, California, 2004.

Lee, T. C., and P. T. Delaney (1987), Frictional Heating and Pore Pressure Rise Due to a Fault Slip, *Geophysical Journal of the Royal Astronomical Society*, *88*(3), 569-591.

Mase, C. W., and L. Smith (1985), Pore-fluid pressures and frictional heating on a fault surface, *Pure Appl. Geophys.*, *122*, 583-607.

Mase, C. W., and L. Smith (1987), Effects of frictional heating on the thermal hydrologic and mechanical response of a fault, *J. Geophys. Res.*, *92*, 6249-6272.

Noda, H. (2008), Frictional constitutive law at intermediate slip rates accounting for flash heating and thermally activated slip process, *J. Geophys. Res.*, doi:10.1029/2007JB005406.

Noda, H., E. M. Dunham, and J. R. Rice (2009), Earthquake ruptures with thermal weakening and the operation of major faults at low overall stress levels, *J. Geophys. Res.*, *114 (B07302)*, doi:10.1029/2008JB006143.

Noda, H., and N. Lapusta (2010), Three-dimensional earthquake sequence simulations with evolving temperature and pore pressure due to shear heating: Effect of heterogeneous hydraulic diffusivity, *J. Geophys. Res.*, *115*, B12314.

Noda, H., and T. Shimamoto (2005), Thermal pressurization and slip-weakening distance of a fault: An example of the Hanaore fault, southwest Japan, *Bull. Seis. Soc. Am.*, *95*(4), 1224-1233.

Rempel, A. W., and J. R. Rice (2006), Thermal pressurization and onset of melting in fault zones, *Journal of Geophysical Research-Solid Earth*, *111*(B9), B09314, doi:09310.01029/02006JB004314.

Rice, J. R. (2006), Heating and weakening of faults during earthquake slip, *Journal of Geophysical Research-Solid Earth*, *111*(B5), doi:10.1029/2005JB004006.

Rice, J. R., and M. Cocco (2007), Seismic fault rheology and earthquake dynamics, in *The Dynamics of Fault Zones*, edited by M. R. Handy, p. in press, MIT Press, Cambridge, Mass.

Rice, J. R., E. M. Dunham, and H. Noda (2010), Thermo- and hydro-mechanical processes along faults during rapid slip, in *Meso-Scale Shear Physics in Earthquake and Landslide Mechanics*, edited by Y. Hatzor, J. Sulem and I. Vardoulakis, pp. 3-16, CRC Press.

Schmitt, S. V., and P. Segall (2009), Thermal pressurization during "slip law" frictional earthquake nucleation, *Poster, 2009 SCEC Annual Meeting*.

Segall, P., and J. R. Rice (2006), Does shear heating of pore fluid contribute to earthquake nucleation?, *Journal of Geophysical Research-Solid Earth*, *111 (B09316)*, doi:10.1029/2005JB004129.

Sibson, R. H. (1973), Interactions between temperature and fluid pressure during earthquake faulting - A mechanism for partial or total stress relief, *Nature*, *243*, 66-68.